

PFC/JA-85-29

ELECTRIC PROBES IN PLASMAS

B. Lipschultz, I. Hutchinson, B. LaBombard, A. Wan

Plasma Fusion Center
Massachusetts Institute of Technology
Cambridge, MA 02139

August 1985

This is an invited paper for the American Vacuum Society 1985 National Symposium. It will be published in the Journal of Vacuum Science and Technology A.

This work was supported by the U.S. Department of Energy Contract No. DE-AC02-78ET51013. Reproduction, translation, publication, use and disposal, in whole or in part by or for the United States government is permitted.

By acceptance of this article, the publisher and/or recipient acknowledges the U.S. Government's right to retain a non-exclusive, royalty-free license in and to any copyright covering this paper.

Electric probes in plasmas

B. Lipschultz, I. Hutchinson, B. LaBombard, and A. Wan

Plasma Fusion Center
Massachusetts Institute of Technology
Cambridge, Massachusetts 02139

This paper provides a background for the use of Langmuir and gridded energy analyzer probes in diagnosing plasmas with varied characteristics. Theory is illustrated which governs the analysis of data from, and the design of these probes. Several probe analysis techniques and some of their typical problems are presented.

PACS numbers: 52.70.Ds; 07.50. + f; 07.50 + x; 06.50.Mk

1. Introduction

Electric and magnetic probes are among the earliest and most basic plasma diagnostics. They are used in a wide variety of plasmas ranging from the low-density, low-magnetic field space plasmas to those at the edge of fusion research devices. Interest in probes has increased and waned over the years since Irving Langmuir first explored their usefulness. They have lately enjoyed a revival in fusion research because of the recently recognized importance conferred upon the plasma edge. Although electric probes are fairly straightforward to design, build and operate, theoretical models used to analyze the resultant data can be quite complicated. Generally, the degree of difficulty encountered in applying the selected model depends on what accuracy is desired.

Choosing a theory depends on two criteria: 1) whether a correct theory exists for the situation in hand, and 2) whether the accuracy and difficulty of performing the theoretical analysis is justified by the accuracy of the experimental data.

This paper presents a brief theoretical background of theory for the operation of, and analysis of data from, Langmuir electric and gridded-energy-analyzer (GEA) probes. Further in-depth theory is available in a number of references.¹⁻⁴ Design criteria and further examples of the use of a variety of probes can be found in the literature.⁵⁻⁷ Perhaps of greater interest to an experimentalist reading this paper is the discussion of various data analysis methods.

2. Simple Probe Theory

2.1 Qualitative Description of the Langmuir Trace

The general form of a Langmuir probe current versus bias voltage characteristic is shown in Fig. 1. In the following discussion, current being drawn by the probe is designated as positive. Φ_p is the plasma potential with respect to the probe ground. When Φ , the probe bias, is very negative with respect to Φ_p , the electric field around the probe will prevent all but the highest energy electrons from reaching the probe, effectively reducing the electron current to zero. The current collected by the probe, I_{si} , is then due entirely to positive ions, which encounter only an attracting electric field; thus it is termed the 'ion-saturation current'.

As Φ is increased, the number of electrons which are able to overcome the repelling electric field and contribute a negative

current increases exponentially, reducing I from the value I_{si} . Eventually, the electron current collected is equal to I_{si} at $\Phi = \Phi_f$. Φ_f is less than Φ_p because the electron thermal velocity is $(M_i/m_e)^{1/2}$ greater than that of the ions. When the probe is allowed to 'float', independent of a bias, it quickly develops the potential Φ_f to repel electrons.

Further increase of the probe bias to Φ_p allows the electron current to completely dominate I . At this probe bias, electrons are completely unrestricted from being collected by the probe. Any further increase in Φ will simply add energy to the electrons, not increase the current drawn. Thus the term 'electron-saturation current' is used in this limit.

2.2 Sheath Analysis for Non-Magnetized Plasmas

When a probe is immersed in the plasma it strongly perturbs the potential over a small region designated the sheath. This perturbation is limited by electron shielding to several Debye lengths ($\lambda_{\text{Debye}} = [\epsilon_0 T_e / n_e e^2]^{1/2}$) in distance from the probe.⁹ The geometry that will serve as a basis for the following discussion is illustrated in Fig. 2. The probe surface is designated by $x = x_p$ and the unperturbed plasma by $x = \infty$. The sheath thickness, $x_s - x_p$, is assumed to be much less than x_p allowing use of a planar approximation, independent of probe geometry. The plasma potential at infinity, $\Phi(\infty)$, is defined to be zero.

The theory of the flow of charged particles to an electrical probe can be extremely complex. In this section we will introduce Langmuir probe theory by way of the simplest case⁸: a probe immersed in a zero-magnetic field plasma with the temperature of

the ions much less than that of the electrons. The following additional assumptions are made about the plasma in which the probe is immersed:

- 1) electron and ion densities are equal;
- 2) Debye length \ll probe dimensions \ll electron and ion mean free paths;
- 3) Maxwellian velocity distributions far away from the probe;
- 4) no bulk motion of the unperturbed plasma ($v_{\text{drift}} \ll v_{\text{thermal}}$);
- 5) no secondary electron emission from the probe surface.
- 6) fully ionized, $z = 1$ plasma.

The task of any probe analysis model is to determine the unperturbed values (in absence of probe) of density and temperature from the measured variation of probe current with changing bias potential. Here, we will concentrate on the range of probe bias where electrons are repelled, i.e. bias potential less than the plasma potential.

A. Density

First let us direct our attention to the electrons. Their density, $n_e(x_1)$, can be obtained by integration over the local distribution function. The relationship of the distribution function at an arbitrary x_1 to that at $x = x_2 = \infty$, can be determined by several factors: first, particles are conserved so that along a particle's trajectory in phase space, $(x_1, v_1) \rightarrow (x_2, v_2)$;

$$f(x_1, v_1) dx_1 dv_1 = f(x_2, v_2) dx_2 dv_2. \quad (1)$$

Second, Liouville's theorem states that the phase volume occupied by a set of 'particles' is constant.¹⁰ In other words $dx dv$ is a

constant allowing us to equate $f(x_1, v_1)$ and $f(x_2, v_2)$. Third, conservation of energy enables us to relate the potential and kinetic energies at the two locations, (x_1, v_1) , (x_2, v_2) , by

$$\frac{1}{2}mv_1^2(x_1) + e\Phi(x_1) = \frac{1}{2}mv_2^2(\infty) + e\Phi(\infty) \quad (2)$$

We can now write down the local distribution function in terms of value at $x_2 = \infty$ and furthermore integrate for $n_e(x_1)$

$$n_e(x_1) = \int_{-\infty}^{v_c} dv_1 n_\infty \frac{m_e}{2\pi kT} \cdot \exp\left[-\left(\frac{mv_1^2}{2} + e\Phi(x_1)\right)/kT\right] \quad (3)$$

For the moment T stands for only the electron temperature. The integration limits are determined by the existence of two classes of electrons: 1) electrons travelling towards the probe ($v < 0$), and 2) electrons that have been repelled before reaching the probe and are travelling away ($0 < v < v_c$). $v_c = \sqrt{2e(\Phi(x_1) - \Phi(x_p))/m_e}$ is the minimum velocity which electrons need to overcome the electric repulsion of the probe and be collected there. Completing the integration we have

$$n_e(x_1) = \frac{n_\infty}{2} \exp(e\Phi(x_1)/kT) [1 + \operatorname{erf}(\sqrt{e(\Phi(x_1) - \Phi(x_p))/kT})] \quad (4)$$

At the x_1 of interest, near the sheath, $\Phi(x_1) - \Phi(x_p) \gg kT/e$ and the Boltzmann relation is retrieved:

$$n_e(x_1) = n_\infty \exp(e\Phi(x_1)/kT) \quad (5)$$

For $x_1 > x_s$ the plasma is quasi-neutral. Therefore Eqs. (4) and (5) apply equally well to ions in that region.

B. Fluxes

Next let us turn our attention to the ion and electron fluxes, and thus the current they carry to the probe. The ion velocity outside the sheath is determined by Eq. (2) where both the unperturbed potential and the ion velocity at $x = \infty$ are defined to be zero. Combining this knowledge with Eq. (5) provides a description of the ion flux outside the sheath region,

$$\Gamma_i(x) = n_i(x)v_i(x) = n_\infty \exp(e\phi(x)/kT) \cdot (-2e\phi(x)/M_i)^{1/2} \quad (6)$$

$(x > x_s)$

where we have dropped the subscript on x . Since there are no particle sources within the sheath, the current flowing to the probe is constant in x . The electron flux to the probe is just the random flux reduced by the Boltzmann factor evaluated at the probe potential, so that the total current collected by a probe at bias $\phi(x_p)$ is

$$I = e \left[-\frac{1}{4} n_\infty \bar{c}_e A_p \exp\left(\frac{e\phi(x_p)}{kT}\right) + A_s n_\infty \exp\left(\frac{e\phi(x_s)}{kT}\right) \left(\frac{-2e\phi(x_s)}{M_i}\right)^{1/2} \right] \quad (7)$$

where A_s and A_p are the sheath and probe areas, x_s the sheath position and \bar{c}_e the electron thermal speed. The potential at the sheath edge, $\phi_s = \phi(x = x_s)$ is as yet undetermined. ϕ_s can be determined by solving Poisson's equation in the vicinity of the sheath.

C. Potential at the Sheath Edge

We now turn our attention to just inside the sheath where ion and electron densities are no longer equal. To determine the ion density for $x < x_s$ we note that in planar geometry, the ion flux

must be constant across the sheath and so

$$n_i(x) = n_{iS}(v_S/v(x)) = n_{iS}\sqrt{\phi_S/\phi(x)} \quad (x \lesssim x_S) \quad (8)$$

where n_{iS} and ϕ_S are the values of ion density and potential at the sheath edge. Then Poisson's equation inside the sheath becomes

$$\nabla^2\phi = -(en_S/\epsilon_0)[(\phi_S/\phi(x))^{1/2} - \exp(e(\phi(x)-\phi_S)/kT)] \quad (9)$$

which, in the region near the sheath, can be expanded⁸ as:

$$\nabla^2\phi = -(en_S/\epsilon_0)\left[-\frac{1}{2\phi_S} - \frac{e}{T}\right](\phi(x) - \phi_S). \quad (10)$$

Non-oscillatory solutions of this equation are possible for $\phi_S \leq -T/2e$. The value of $d\phi/dx$ for $x \gtrsim x_S$ can be obtained from Poisson's equation in the quasineutral region outside the sheath.³ $\phi(x)$ has infinite slope for $\phi_S \geq -T/2$. Therefore we determine that

$$\phi_S = -T/2e. \quad (11)$$

There are no solutions of Poisson's equation (no sheath) for $\phi(x_p) > -T/2e$.

D. Total Current to Probe

Substituting the value for the sheath potential, Eq. (11), into Eq. (7), the current collected by the probe is then

$$\begin{aligned} I &= I_{se}\exp(e\phi(x_p)/kT) + I_{si} \\ &= -eA_p[1/4n_\infty\bar{C}_e \cdot \exp(e\phi(x_p)/kT) - n_\infty(T_e/M_i)^{1/2}\exp\left(-\frac{1}{2}\right)] \end{aligned} \quad (12)$$

$$I_{se} = -eA_p(1/4n_\infty\bar{C}_e) \quad (13)$$

$$I_{si} = .61n_{\infty}C_sA_p e \quad (14)$$

The sheath area has been taken to be approximately equal to that of probe. C_s is the ion sound speed. The floating potential can be solved for by setting Eq. (12) to zero:

$$e\phi_f/T_e = .5[\ln(2\pi m_e/M_i) - 1] \quad (15)$$

T_e can be obtained by examining the slope of the curve described by Eq. (12) in the exponential region between I_{is} and I_{es} . Then the density can finally be deduced from Eq. (14).

Throughout this discussion we have effectively assumed the ion temperature should be low enough such that $0.5M_i v^2(\infty) \ll -e\phi(x_p)$. If finite ion temperature is allowed at $x = \infty$, then the specific ion orbits and probe geometry must be included in the model. No simple formulae exist for replacing Eq. (14) because of the numerical integrations involved, but some results indicate a weak dependence of the constant $.61(=e^{-1/2})$ in that formula. Results for monoenergetic ions with $T_i = .01 \cdot T_e$ and $.5 \cdot T_e$ incident on a spherical probe⁴ yield coefficients of .57 and .54 respectively. Therefore, in practice, Eq. (14) is widely used.

3. Refinements to Langmuir Probe Theory

3.1 Practical approach to probe theory with non-zero magnetic field

The above theory is even further complicated by the inclusion of magnetic field effects. Ions and electrons spiral around the magnetic field lines with a radius, in the plane perpendicular to the field line, of $r_l = mv/eB$. If this Larmor radius for both ions and electrons is much greater than the probe dimension, a , then the previous zero-magnetic field results are recovered.

The determination of T_e can be divided into three regimes: $r_{1e} \gg a$; $r_{1e} \ll a$; $r_{1e} \sim a$. The first, as described above, is equivalent to that of the unmagnetized plasma. In the second regime, one must assume that the electron term of Eq. (12) is unaffected other than a fractional reduction (R) of the current due to the limiting rate of cross field diffusion.

$$I_e = R \left[- \frac{1}{4} n_{\infty} \bar{C}_e \exp(e\phi(x_p)/kT_e) \right]; \quad 0 < R < 1 \quad (16)$$

Such a reduction parameter was derived by Bohm.⁴ R decreases as some monotonic function of the ratio of perpendicular to parallel diffusion coefficients. Such an effect can be brought about by increasing magnetic fields or with large sized probes.¹³ Eq. (16) allows T_e to be deduced in the usual fashion.

In the remaining regime, $r_{1e} \sim a$, T_e should be determined by fitting Eq. (12) to the data only over that portion where $r_{1e} < a$.

Once T_e is determined from the above recipes, then the unperturbed density, n_{∞} , follows from Eq. (14) assuming, for $r_{1i} < a$, that the probe area is reduced to its projection along the magnetic field.

3.2 Analytic result for non-zero magnetic field, $T_i \sim 0$

An analytic treatment of probes in a high magnetic field plasma similar to that outlined in section 2 does exist.¹¹ Collisions are allowed sufficient to provide the minimum particle source required to make this one-dimensional problem soluble. Too many collisions causes an ion to lose its memory of the potential where it was borne along the potential gradient. The values of the sheath potential, ion flux and floating potential are modified

as follows:

$$\phi_S = -0.854 \cdot T_e/e \quad (17)$$

$$\Gamma_i = A_S n_\infty (2T_e/M_i)^{1/2} (1/\pi) \phi_S^{-1/2} = .49 n_\infty C_S A_S \quad (18)$$

$$\phi_f = (T_e/2e) \ln(4m_e/\pi M_i) \quad (19)$$

A_S is again the projected area of the sheath along the field line. Although the sheath potential is significantly modified with respect to the zero-magnetic field results, the coefficient for the ion-saturation current is not. Given the accuracy of typical probe data, a coefficient of .5 in Eqs. (14) and (18) is adequate for most cases, except perhaps when the ion flux is reduced by limits on perpendicular diffusion into the probe flux tube.

3.3 Non-zero magnetic field, $T_i > 0$

A kinetic treatment of the general case of strong magnetic fields and a range in T_i is given by Emmert.¹² Unfortunately the assumption that ions are borne with non-negligible ion temperature leads to unphysical results for $T_i \gg T_e$. In this limit, the predicted ion flux to the surface becomes twice the random value. The calculation of the sheath potential, however, is probably reliable.

Possibly the most general theory that can be applied to the variety of situations outlined above is that of Stangeby.¹³ This approach, in contrast to others discussed, is a fluid treatment which is not rigorously correct in a nearly collisionless regime. Nevertheless, most results obtained by kinetic treatments can be reproduced by this model in the appropriate limits. The primary attraction of this model is from an application point of view.

It purports to cover the complete range of non-magnetized to magnetized plasmas.

4. Gridded Energy Analyzer (GEA) Analysis

The Langmuir probe is a small but rugged diagnostic for determining electron temperatures, through the electron distribution function Eq. (12), and ion densities. Unfortunately it cannot be used to determine the ion temperature nor the existence of non-thermal components in either species.

The GEA complements the Langmuir probe because of its ability to measure those different parameters as well as T_e . What is sacrificed in going to this type of probe is small probe size and a straightforward density measurement. Examples of its use are found in the work of Matthews¹⁴ and others.¹⁵⁻¹⁷

A typical GEA geometry is shown in Fig. 3a. The entrance to the GEA can either be a grid or a more rugged knife-edge slit depending on particle and heat flux considerations. The purpose of the entrance aperture is to produce a sheath which simultaneously reduces the electron heat flux to the interior of the analyzer and retains the Maxwellian nature of the ion distribution function.¹² In other words the aperture should be small enough to allow the sheath potential perturbation due to the presence of the detector to extend uniformly across the slit, but large enough to allow a detectable flux to enter. The entering current would then be that of Eq. (12) with the same caveats (that $\phi_{\text{plasma}} - \phi_{\text{slit}} > \phi_{\text{sheath}}$). The slit width or grid spacing should be less than $10 \cdot \lambda_{\text{debye}}$, or roughly two times the sheath perturbation distance, to achieve this result.

A diagram describing the potential at each grid biased for the measurement of ion temperatures is shown in Fig. 3b. The first grid, G_1 , is used to repel the unwanted species, in this case electrons. The bias, ϕ_2 , of the second grid, G_2 , is then varied to limit the collection of ions to those with unperturbed velocity ($x = \infty$) less than $v_c = -\sqrt{2e(\phi_2 - \phi_{\text{plasma}})/M_i}$. The last grid is biased to suppress secondary electron emission from the collector. For measurement of the electron temperature, most ions must be repelled. G_1 should be biased such that $\phi_1 > \phi_{\text{plasma}} + \delta \cdot T_i, \delta \gg 1$. ϕ_2 is varied negative with respect to ϕ_{slit} to 'sweep out' the electron distribution function.

To determine the temperature of either species one examines the variation of current drawn at the collector with varying G_2 bias similar to the determination of T_e from a Langmuir probe trace. Specifically, in determining T_e , when ϕ_2 is negative with respect to ϕ_{slit} , the electron current collected will just be the standard Langmuir electron current:

$$I = -e \cdot TF(\text{electrons}) A_{\text{slit}} (1/4n_{\infty} \bar{C}_e) \exp(\phi_2 - \phi_{\text{plasma}}) \quad (20)$$

where TF is the transmission factor of the grids. The exponential term is just the Boltzmann factor for the reduction in the random electron flux. For the purposes of obtaining T_e , Eq. (20) can be rewritten

$$I = I_0 \exp(e(\phi_2 - \phi_{\text{slit}})); \quad \phi_2 < \phi_{\text{slit}} \quad (21)$$

The ions are only slightly more complicated:

$$\begin{aligned}
 I &= TF(\text{ions})eA_{\text{slit}}(.5n_{\infty}C_S)\exp[-e(\phi_2 - \phi_{\text{plasma}})/kT_i]; \\
 &\hspace{15em} \phi_2 \geq \phi_{\text{plasma}} \\
 &= TF(\text{ions})eA_{\text{slit}}(.5n_{\infty}C_S); \hspace{15em} \phi_2 \leq \phi_{\text{plasma}}
 \end{aligned}
 \tag{22}$$

Again we have assumed $|\phi_{\text{plasma}} - \phi_{\text{slit}}| > |\text{sheath potential}|$ and that the ion flux entering the aperture is $.5n_{\infty}C_S$ with a minimum parallel velocity of $\sqrt{2e(\phi_{\text{plasma}} - \phi_{\text{slit}})/M_i}$.

The primary drawback of the GEA probe is its size which necessarily creates a larger perturbation than a Langmuir probe. The distance between the entrance slit and the leading edge of the GEA housing limits the amount of plasma that can be sampled. Estimation of the unperturbed density is much more complicated than for a Langmuir probe. Transmission factors, which are energy and species dependent, must be calculated with the use of Monte-Carlo methods to follow individual particle orbits.^{14,15} The perturbing effect of such a large structure must also be taken into account.¹³

5. Fitting Techniques and Practical Considerations

In this section the subject of fitting the above models to the data is addressed. For most cases, the comments pertaining to Langmuir probes are equally applicable to the GEA so that explicit references to the GEA analysis will be limited to some examples in section 5.3.

5.1 Logarithmic determination of T_e

The advantage of this technique is its simplicity. An estimate of I_{sat} is made utilizing the knowledge that it is equal

to the total current collected at large negative biases. The estimated I_{sat} is then subtracted from the current measurements at probe voltages, $\phi < \phi_{\text{plasma}}$, Fig. 1, leaving only the exponential portion of Eq. (12). T_e is determined by fitting a straight line to the logarithm of that difference. Appropriate transformation of the data weighting must be included¹⁸ in the least-squares fit. Once T_e is determined, the ion density is calculated using the estimated value of I_{sat} and Eq. (13).

There are several obstacles implicit in obtaining T_e in this fashion from a Langmuir trace. The ion-saturation current is estimated by averaging current measurements in some appropriate voltage region. Similarly, the fit to the exponential part of the trace must also be limited to a range of points below electron-saturation and above the voltage where $(I - I_{\text{sat}})$ is on the order of the uncertainty in I_{sat} . These limits must be determined at the initiation of the fitting procedure. In practice the upper-voltage limit to ion-saturation, V_{is} , is usually predetermined by external input. V_{es} , the voltage at the onset of electron-saturation, which can be set equal to the upper-voltage limit to the exponential fit, can be determined visually by the appearance of a 'knee' in the collected current above V_{is} .

A numerical algorithm can also be used to determine the 'knee' in the $\ln(I)$ plot, Fig. 4. A first value of V_{es} should be guessed either from pre-analysis input or from a previous time-step fit. Then, straight lines are fitted to $\ln(I - I_{\text{sat}})$ on either side of it. The intersection of those two lines provides a new guess for

V_{es} . The iteration is continued until the change in V_{es} from one iteration to the next is less than some predetermined parameter.

Let us consider how accurate this determination of T_e is. We have estimated I_{sat} by an average over k data points where the electron current is approximately zero. The error in determining I_{sat} is then ϵ/\sqrt{k} , where ϵ is the average signal uncertainty. If those points where $(I-I_{sat})$ is of order ϵ/\sqrt{k} are included in any linear fit to the logarithmically transformed data, the slope will be flatter than $1/T_e$, thus overestimating the value of T_e .

The error in I_{sat} can be reduced by increasing k , the number of data points with current in ion-saturation. If the digitization rate is held constant, the result of increasing k is that either the time resolution is degraded or the number of data points used to determine T_e is reduced.

There is one extra step that can be undertaken in pursuing better accuracy in I_{sat} and T_e by this technique. After determining the limits in voltage over which the logarithmic fit should be applied, the value of I_{sat} and thus T_e can be iterated, based on the deviation of the data from the fitted line. The deviation of the data will change in sign depending on the sign of the difference between 'real' and guessed I_{sat} . The merits of performing these extra iterations are dubious in light of the minimal gain in accuracy and the advantages of the exponential fit which will be described next. An example of the logarithmic fit to one Langmuir trace, without this last iteration, is shown in Fig. 5.

5.2 Exponential fit

A more accurate, but minimally more complicated technique is to fit I_{sat} and T_e simultaneously. After finding the 'knee' in the data at V_{es} , as outlined in section 5.1, the data for lower bias voltages can be analyzed by a least-squares fit to a version of Eq. (12)

$$I = I_{\text{sat}} + b \exp(-V/kT_e) \quad (23)$$

which is linear in b and I_{sat} , but non-linear in T_e . If we define $Z(V, T_e) = \exp(-V/kT_e)$ then I_{sat} and b can be solved for in terms of T_e through the usual linear least-squares fit. Therefore, in practice, the nonlinear least squares fit to all three parameters can be found by iteration on one (T_e). This technique fits the data with uniform weighting and negates the need for a large number of data points at large negative bias. Results for an exponential fit are also shown in Fig. 5.

A version of the above exponential fit can be used to apply the Stangeby probe model¹³ to Langmuir probe data.¹⁹ Unfortunately, the process is significantly more complicated. In addition, the benefits gained by choosing said model are questionable.¹⁹

5.3 GEA fit

As discussed in the beginning of section 4, the fit to GEA data is very similar to that for Langmuir probes. First let us discuss the case of determining the ion temperature. A plot of ion current versus positive G_2 bias is shown in Fig. 6a. There is a 'knee' in this data, corresponding to $\phi_2 = \phi_{\text{plasma}}$ (Eq. (22)), below which the current is unaffected by bias. This is

because the ions are 'borne' with the plasma potential far away from the probe. After determining this 'knee' voltage in the fashion described earlier, the ion temperature can again be fit either by logarithmic or exponential methods.

A plot of electron current versus G_2 bias is shown in Fig. 6b. There is no need to find a 'knee' in this curve as per the Langmuir probe analysis. All of the data shown should be useful in determining T_e . A direct fit by either logarithmic or exponential methods is appropriate. In fact, the logarithmic fit should be simpler for the GEA than for Langmuir probes if for large negative G_2 bias, the collected current reduces to zero as it should.

In the case of a non-thermal component or two-temperature population the GEA analysis becomes significantly more complicated. Care must be taken to increase the magnitude of the G_2 bias swing to appropriately reduce the collected current to zero. Then an iterative technique, assuming knowledge of the temperature of one component to fit the other is repeated until convergence.

5.4 Bias Voltage Waveforms

To maximize the time resolution of the analyzed probe data, it is useful to examine the relative merits of different waveforms for biasing the Langmuir probe or GEA. Short period voltage sweeps increase the time resolution of the analyzed data, but also increase the uncertainty of the result due to fewer data points. The error signals caused by stray-capacitance-induced displacement currents are also increased. In practice, most of

the induced error signal can be subtracted at the initiation of data analysis.

The number of points sampled with the probe in ion-saturation, exponential or electron-saturation during a single sweep is transformed by the bias voltage waveform. A sinusoidal waveform has the advantage of only one frequency component, but the disadvantage of sampling the greatest number of points in electron and ion saturation. A triangular, or sawtooth sweep is a better choice from this point of view. It is also easily generated by analog waveform generators, and a greater percentage of the data is taken in the exponential part of the Langmuir trace. An even greater fraction of the data can be taken in the exponential part of the Langmuir trace if the experimenter has the ability to digitally preprogram more 'exotic' bias waveforms. $V(t) = \arcsin(t)$, for $-1 \leq t \leq 1$, is such an example. It is particularly well suited for the determination of T_e by the exponential fitting technique of section 4.2.

Such flexibility in generating waveforms can also be applied to GEA grid biases as well. For example, G_1 and G_2 can alternate from one sweep to the next, between bias potentials needed to measure ion and electron temperatures.¹⁵

6. Summary

Theory that provides an exact description of the operation of a given probe can be quite complicated. However, in practice, several simple formulae reviewed in this paper can be applied with reasonable accuracy. Numerical algorithms are also outlined which can provide efficient computer analysis of Langmuir probe and GEA data.

Work supported by U.S. Department of Energy Contract No. DE-AC02-78ET51013.

References

- ¹J.D. Swift and M.J.R. Schwar, 'Electric Probes for Plasma Diagnostics' (Iliffe Books, London, 1971).
- ²F.F. Chen, in 'Plasma Diagnostic Techniques', edited by R.H. Huddlestone and S.L. Leonard (Academic Press, New York, 1965).
- ³P.M. Chung, L. Talbot, and K.J. Touryan, 'Electric Probes in Stationary and Flowing Plasmas' (Springer-Verlag, New York, 1975).
- ⁴D. Bohm, 'The Characteristics of Electrical Discharges in Magnetic Fields' (McGraw-Hill, New York, 1949).
- ⁵D.M. Manos, J. Vac. Sci. Technol. A, to be published.
- ⁶P. Staib, J. of Nucl. Mat., 111 & 112, 109 (1982).
- ⁷G.M. McCracken, 'Wall and Limiter Diagnostics for Fusion Reactor Conditions', Vol. 11, Varenna, 419 (1982).
- ⁸I.H.H. Hutchinson, 'Plasma Diagnostics', to be published.
- ⁹F.F. Chen, 'Introduction to Plasma Physics' (Plenum Press, New York, 1974).
- ¹⁰K.R. Symon, 'Mechanics' (Addison-Wesley, Reading, 1960).
- ¹¹E.R. Harrison and W.B. Thompson, Proc. Phys. Soc. London, 74, 145 (1959).
- ¹²G.A. Emmert, R.M. Wieland, A.T. Mense, and J.N. Davidson, Phys. Fluids, 23, 803 (1980).
- ¹³P. Stangeby, J. Phys. B, 15, 1007 (1982).
- ¹⁴G.F. Matthews, J. Phys. D: Appl. Phys., 17, 2243 (1984).
- ¹⁵A.S. Wan, Bull. of Amer. Phys. Soc., 29, 1223 (1984).

- 16A. Molvik, Rev. Sci. Inst. 52, 704 (1981).
- 17H. Kimura, et al., Nucl. Fusion, 18, 1195 (1978).
- 18P.R. Bevington, 'Data Reduction and Error Analysis for the Physical Sciences' (McGraw-Hill, New York, 1969).
- 19B. LaBombard, 'Poloidal Asymmetries in the Alcator C Edge Plasma', soon to be finished.

Figure Captions

1. Standard Langmuir trace of current drawn to the probe versus probe bias.
2. Illustration of potential perturbation caused by a probe.
3. Gridded Energy Analyzer geometry (a), and grid bias (b) for measurement of ion temperature.
4. Determination of V_{es} , the onset of electron saturation. Circles are the data, lines are fits to the data above and below V_{es} .
5. Langmuir trace: circles are the data, solid line is the logarithmic fit, broken line, the exponential fit.
6. GEA data: for measurement of ion (a) and electron (b) temperatures. Circles are the data, solid line the exponential fit.

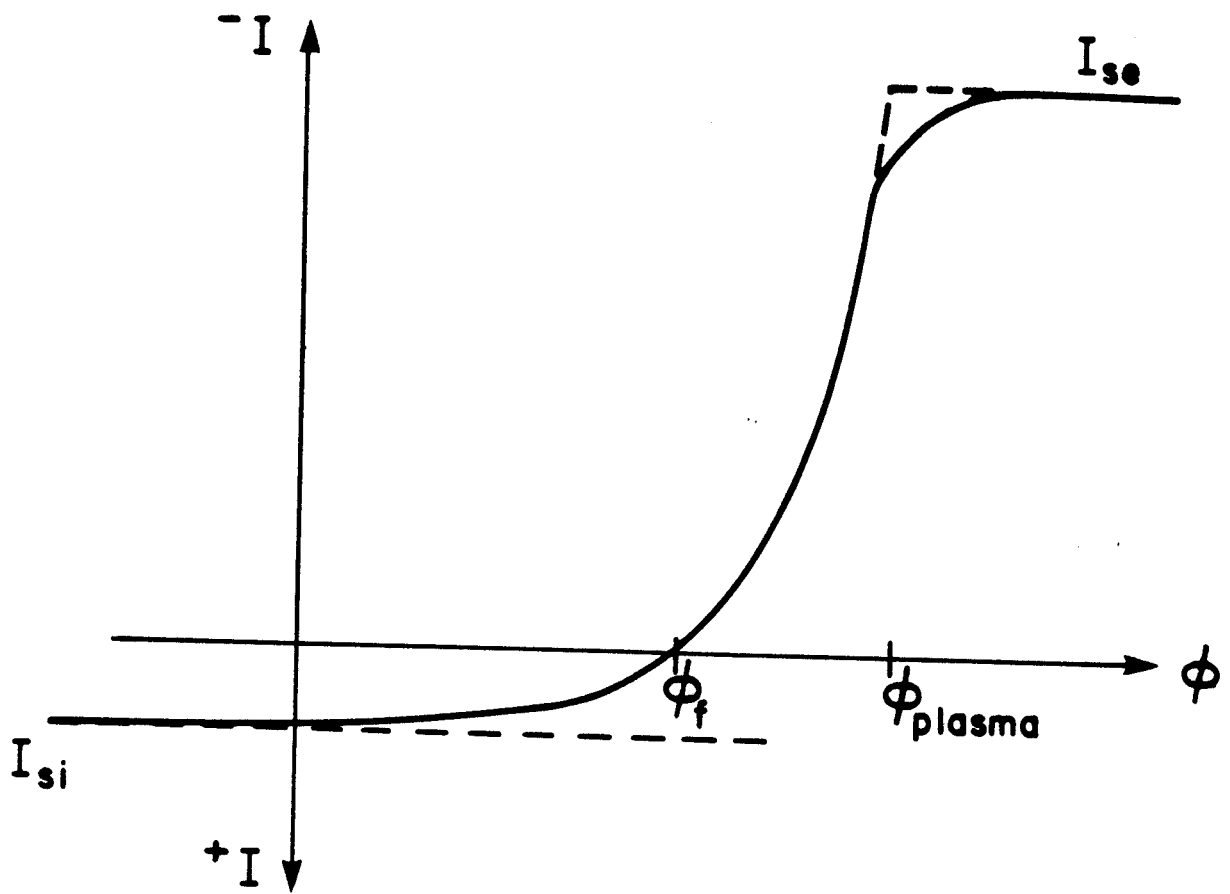


FIGURE 1

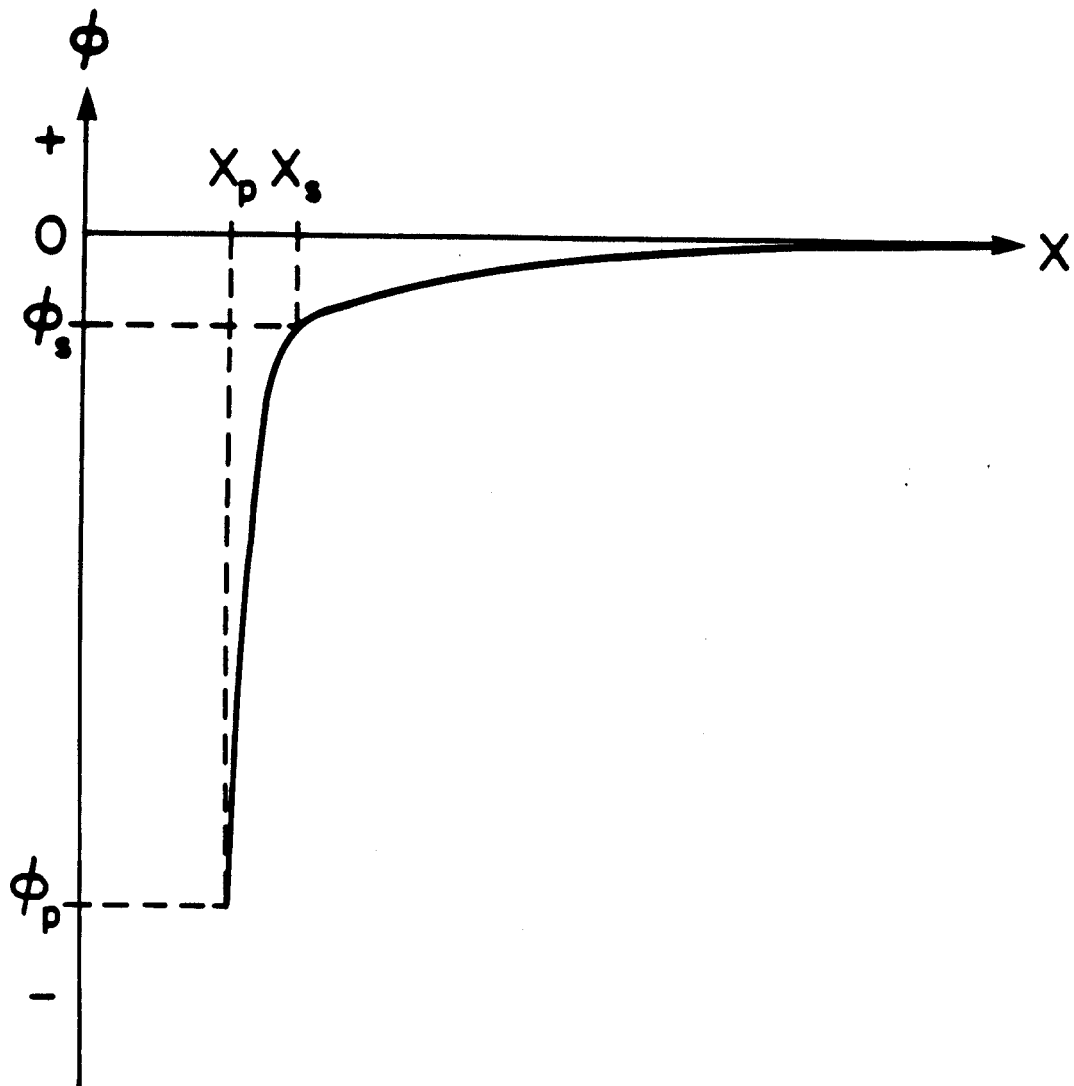


FIGURE 2

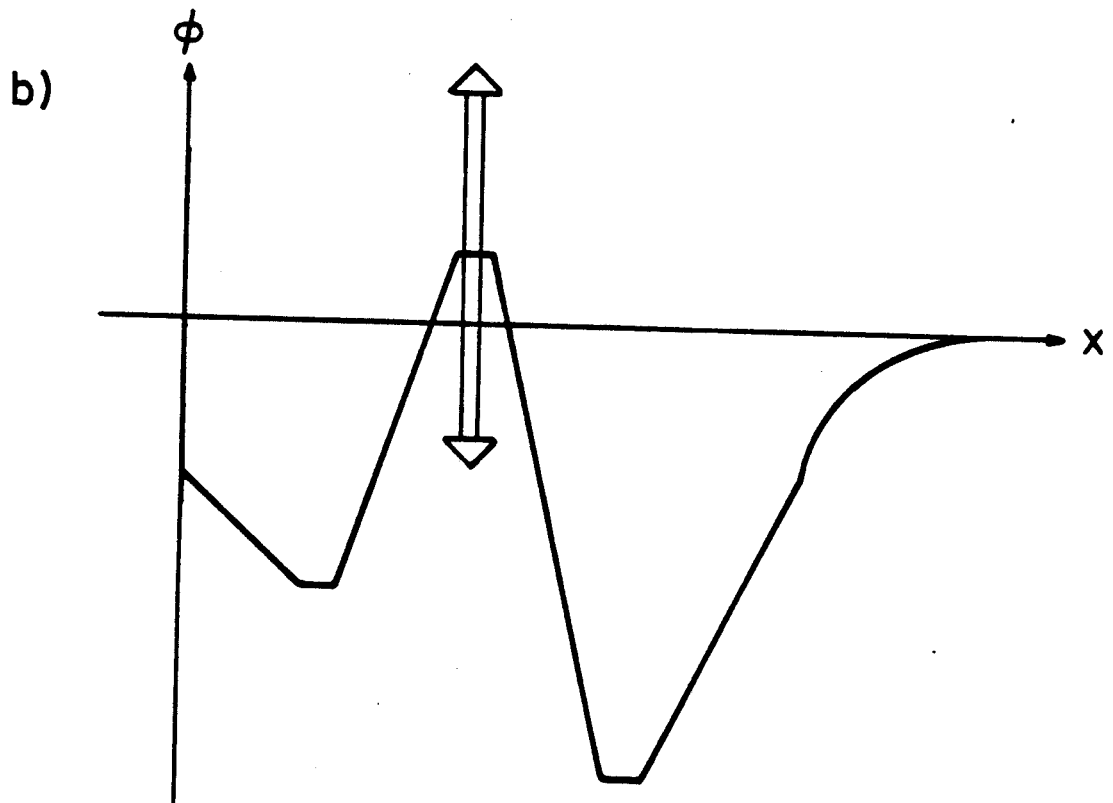
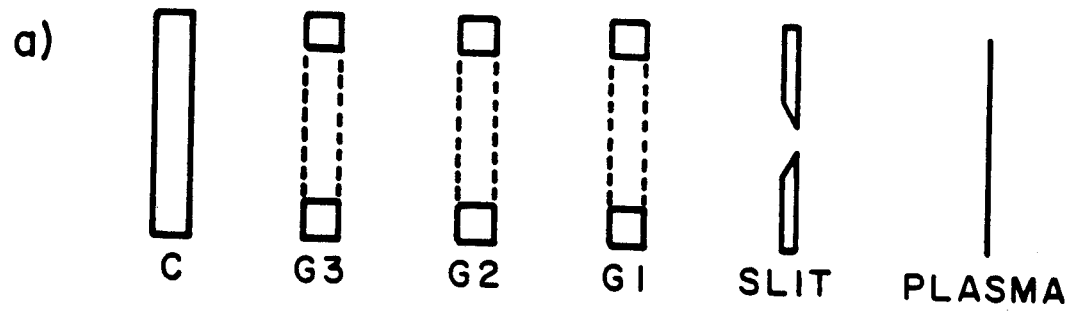


FIGURE 3

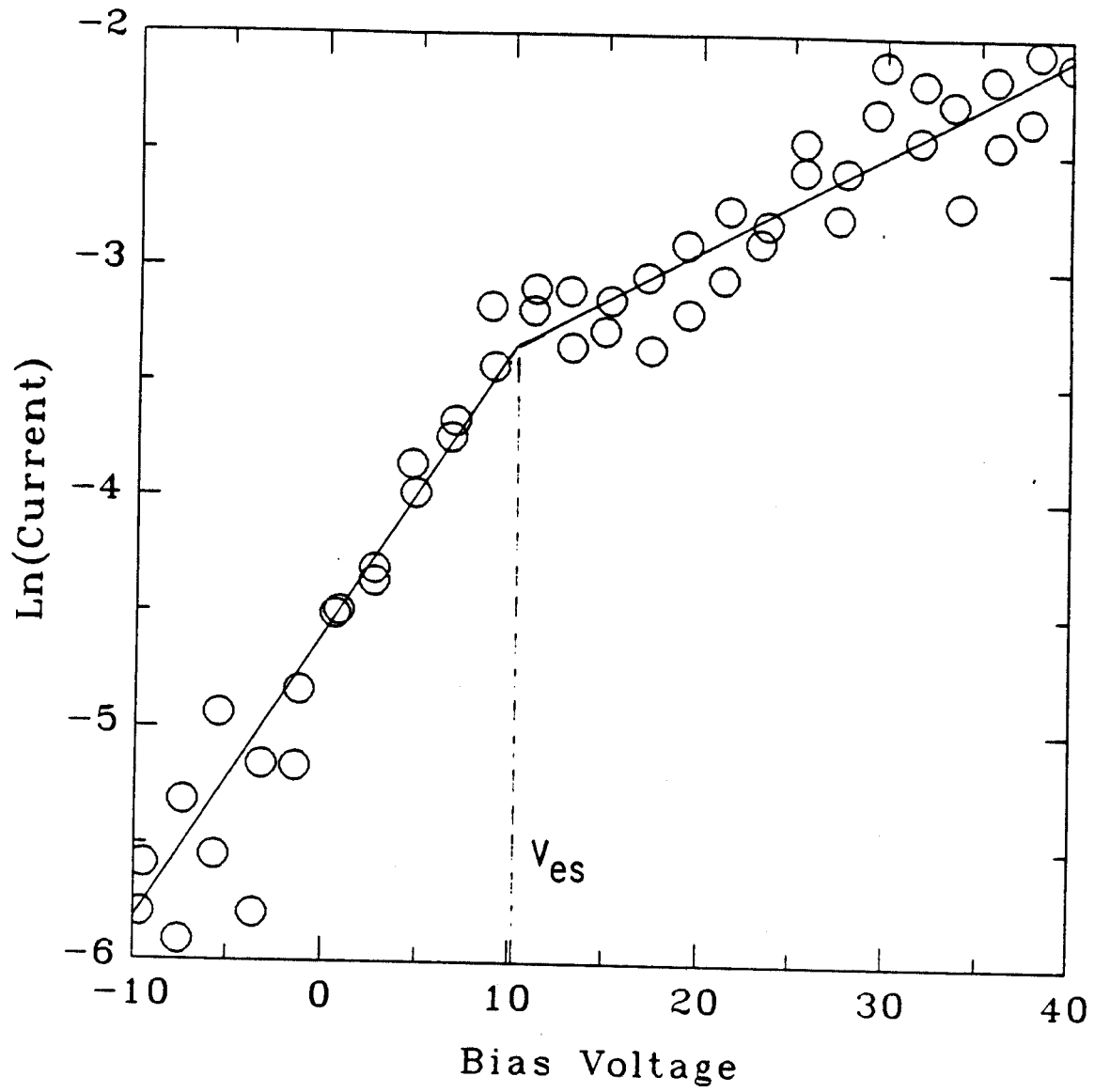


FIGURE 4

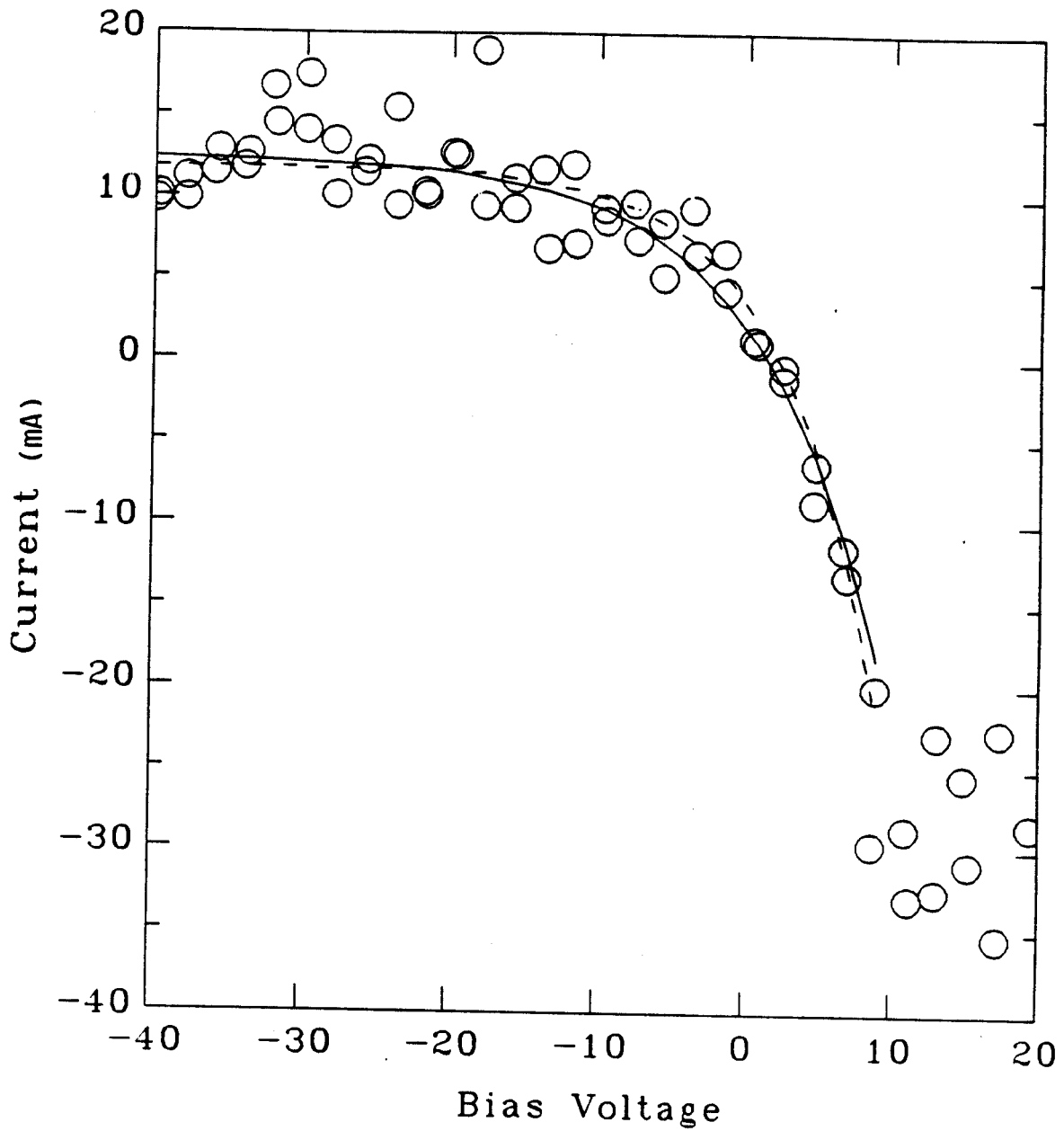


FIGURE 5

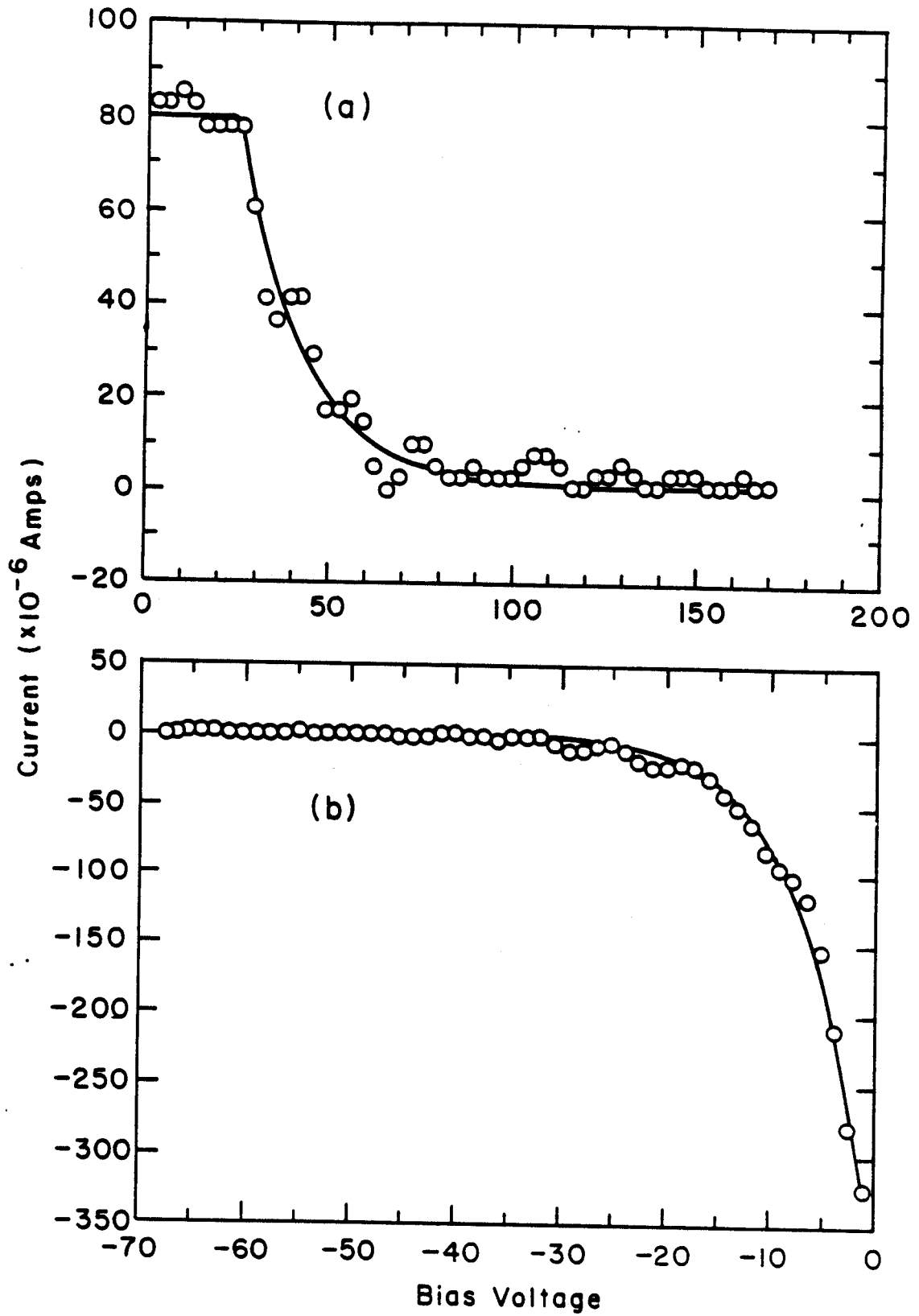


FIGURE 6